Thermal Infrared Image of Effluent Entering the Savannah River Swamp System

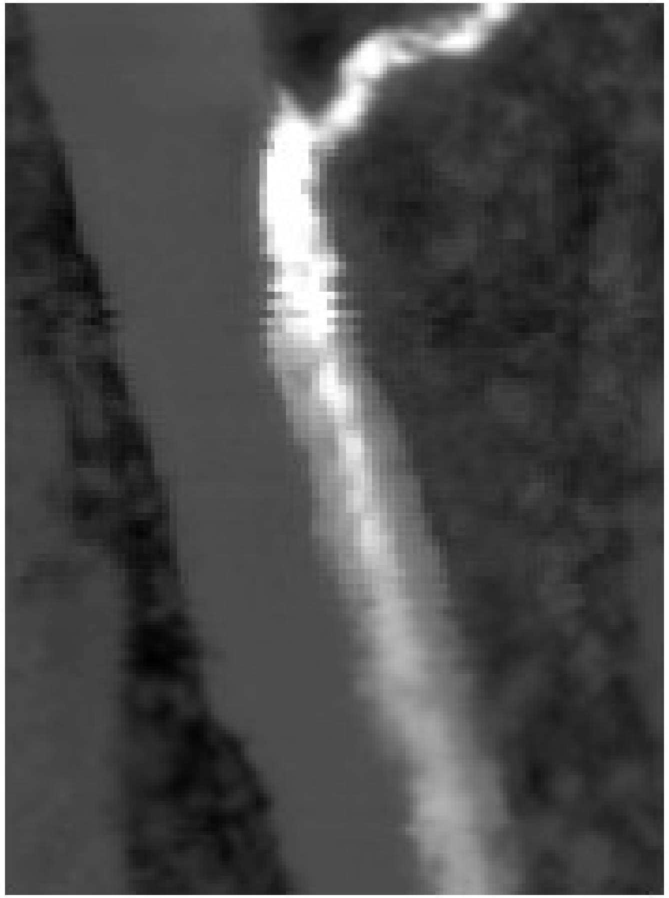

Sea Surface Temperature

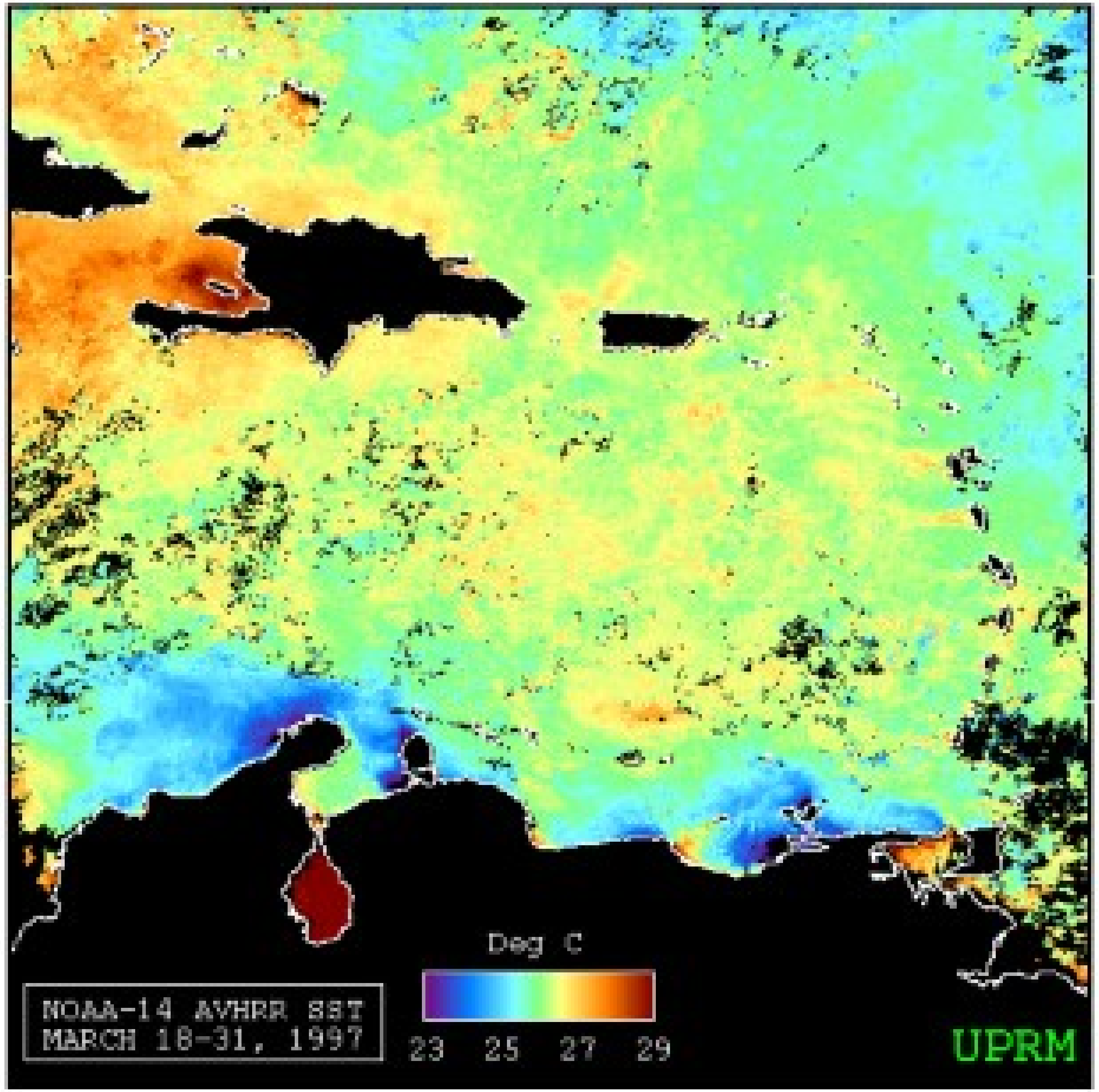

LAKE SUPERIOR

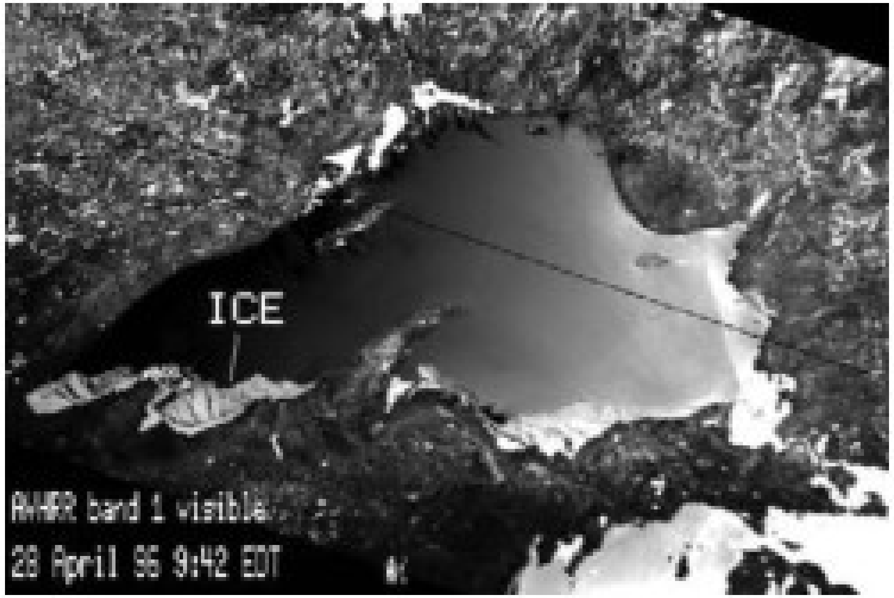

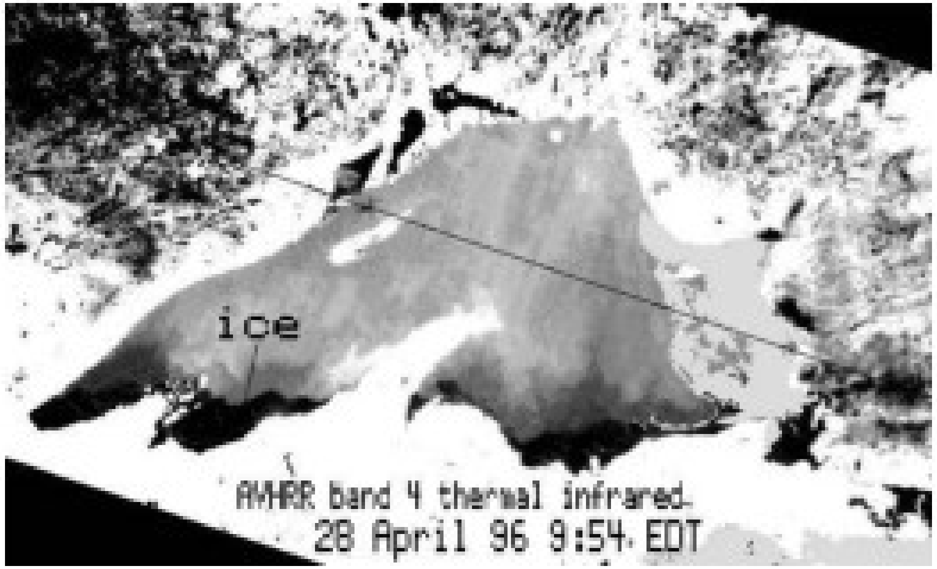

Nighttime Thermal Infrared Imagery of an Airport

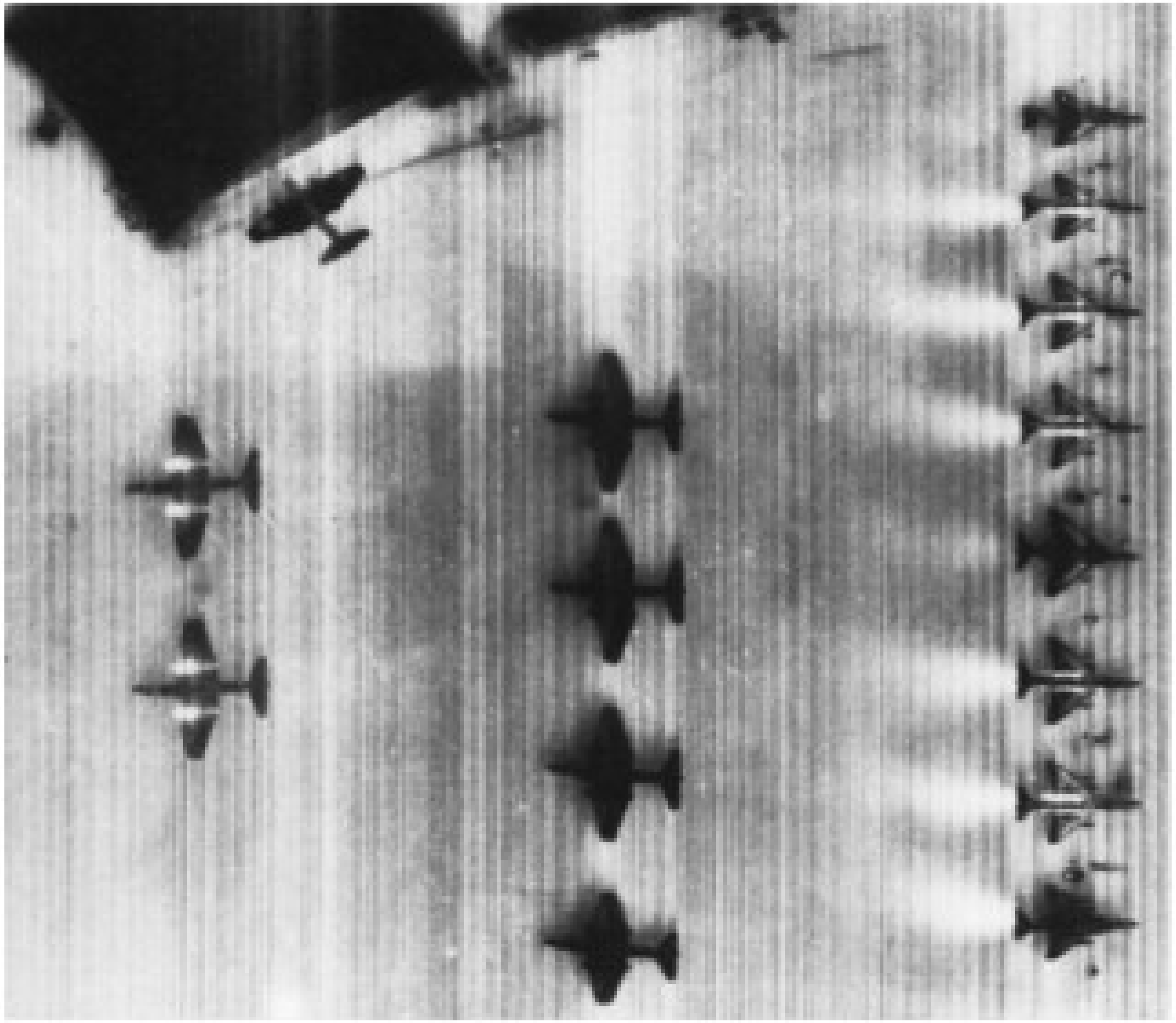

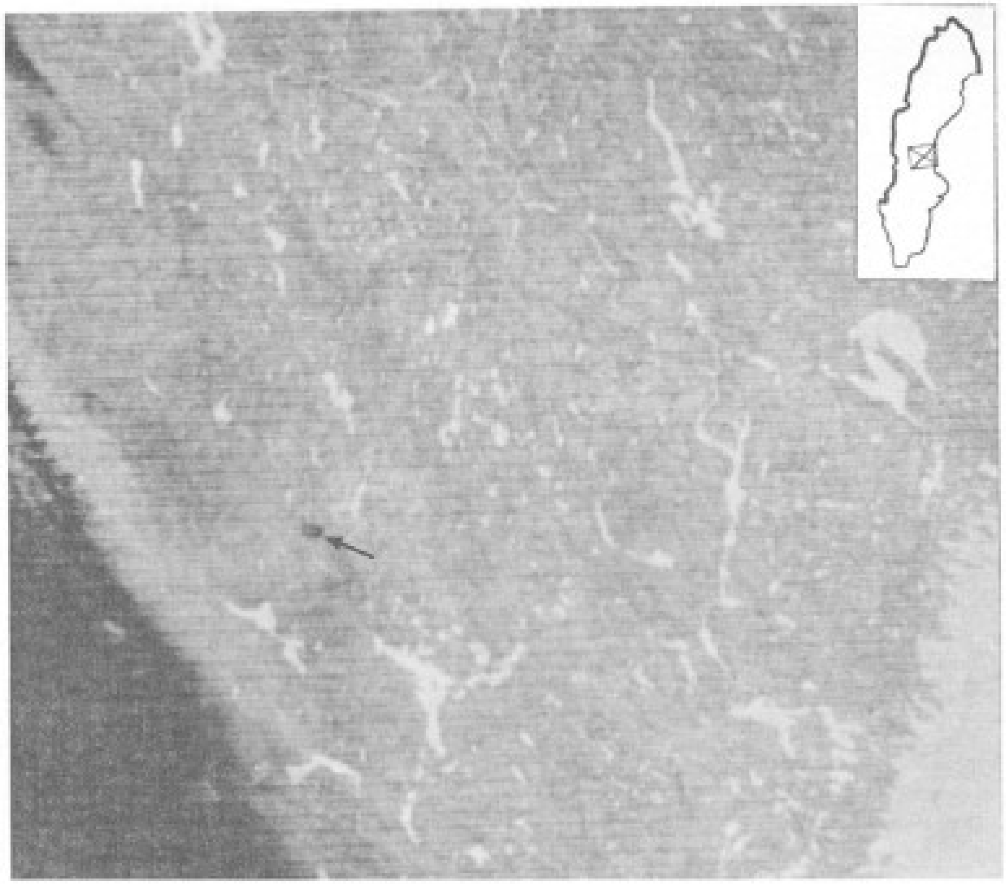

Fig. 1. The Landsat TM thermal image used in this study, from 11 October, 20.40, and covering an area approx. 180 by 180 km. The grey tones in the image are related to the temperatures of the emitting objects; light toned areas are warmer than the areas with dark grey tones. Clearly visible is the, compared to the land areas, relatively warm lake and sea water, and a cold cloud front coming in from southwest. For more details, see text.

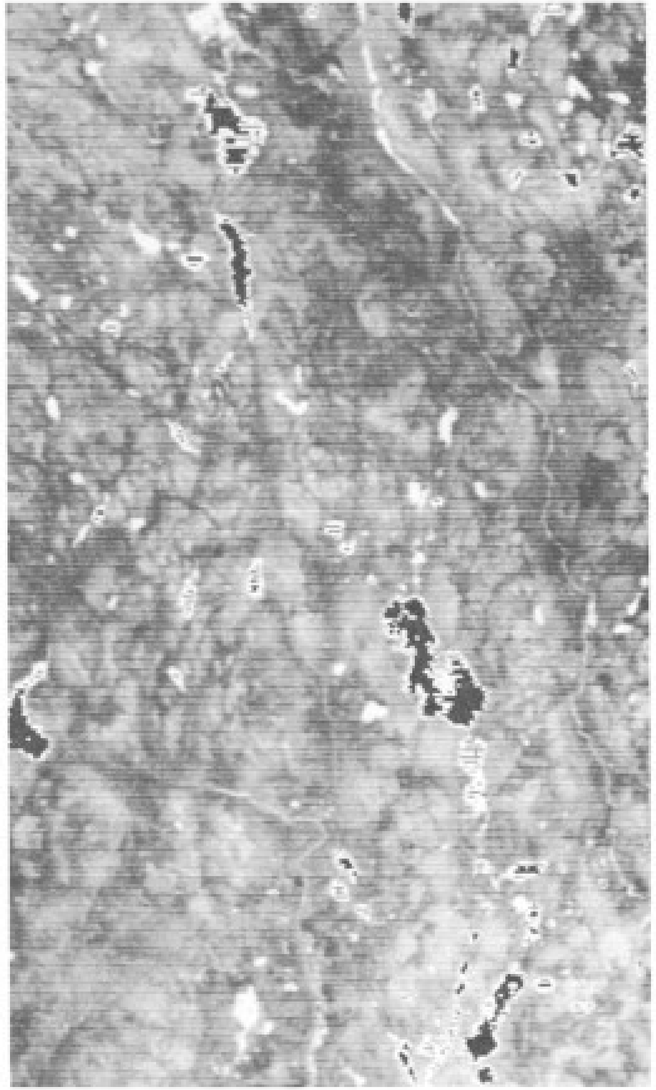

Fig. 2. Sub-scene, covering an area approx. 40 by 60 km, from the central part of the Landsat TM thermal image shown in Figure 1. Light grey tones correspond to warmer areas than dark tones. Within this sub-scene the clear- cut study was carried out, and ground-based temperature measurements were made during the night of the satellite pass. Lake water pixels, for which the TM digital value correspond to a real (corrected for atmosphere and emissivity) temperature of 4±1.0°C, are here especially enhanced and presented in a black tone. For more details, see text.

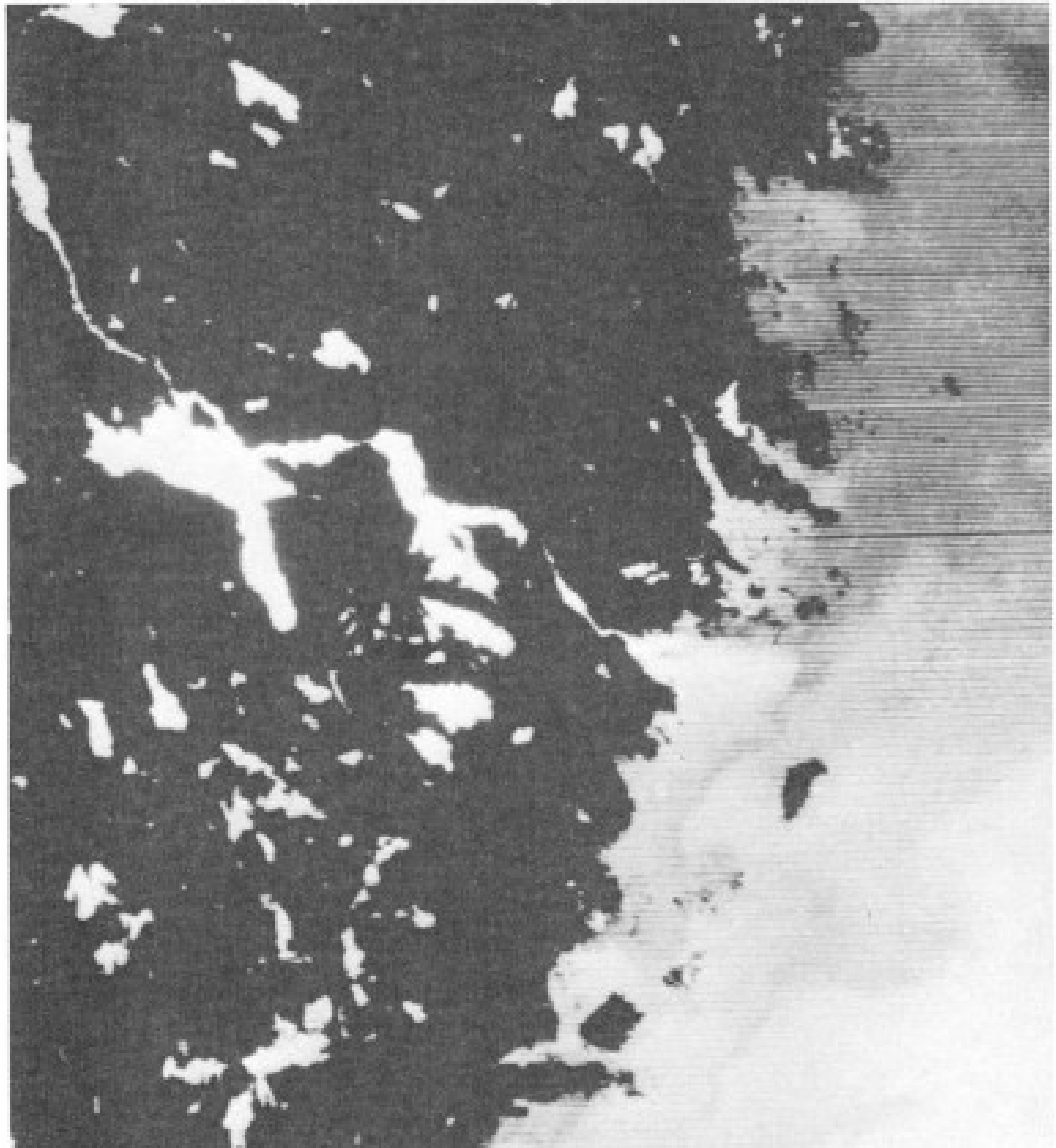

Fig. 3. Sub-scene, approx. 50 by 60 km, of the thermal imagery shown in Figure 1 over a part of the coastal area. Light grey tones correspond to warmer areas than dark tones. This image is stretched to maximally display the temperature pattern of the water areas, which results in a reduced information about the temperatures of the relatively cold land area. For more

On April 5 ASTER captured this night time thermal infrared image of Mt. Usu. Hot thermal anomalies, appearing as bright spots, are seen on the west flank of Usu, site of the eruptions. Additional hot spots appear at the summit, and at a vent on the east flank.

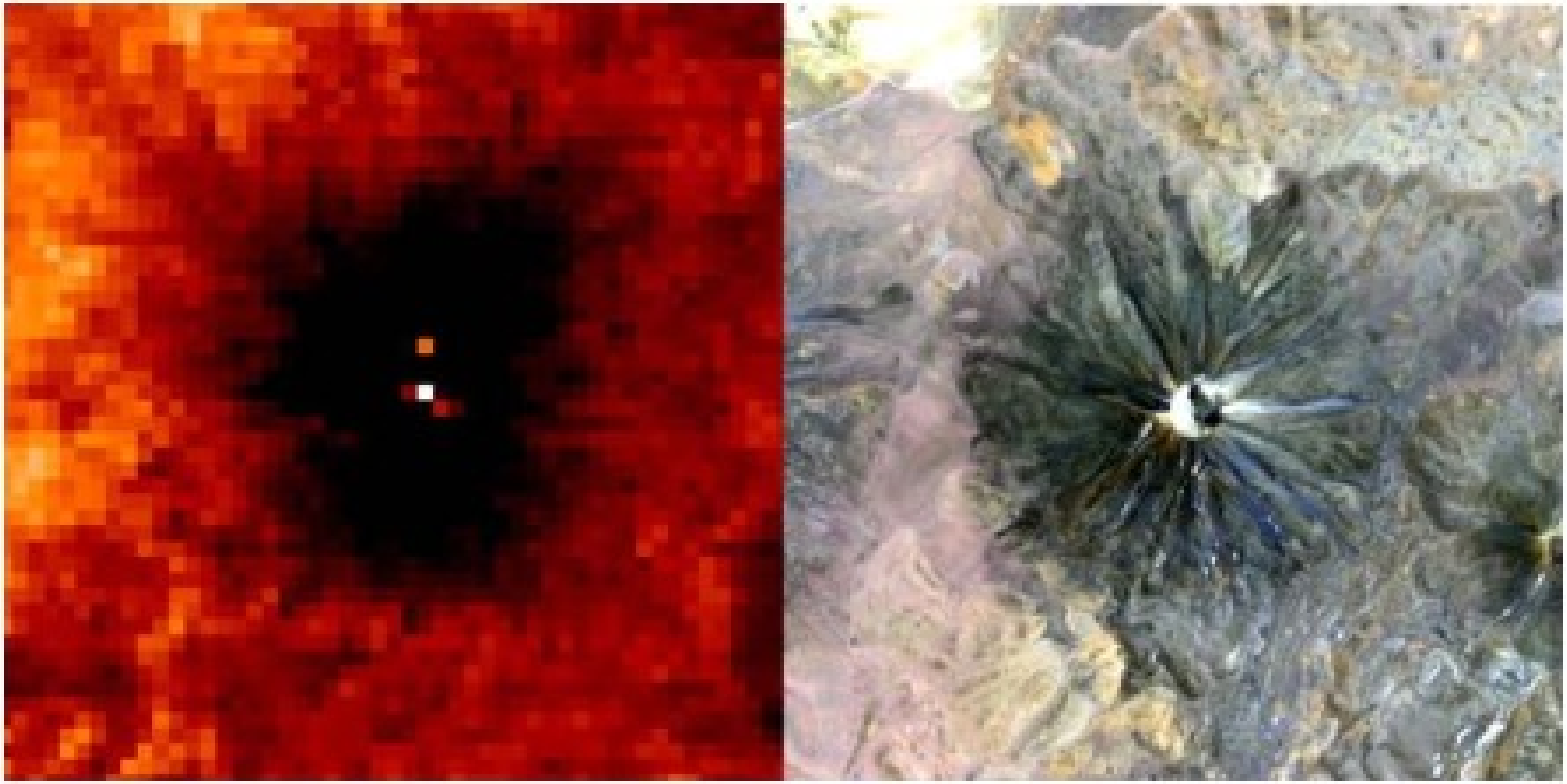

LEFT: A January 6, 2002 ASTER nighttime thermal infrared image of Chiliques volcano in Chile shows a hot spot in the summit crater and several others along the upper flanks of the edifice, indicating new volcanic activity.

RIGHT: The daytime image was acquired on November 19, 2000 and was created by displaying ASTER bands 1,2 and 3 in blue, green and red. The nighttime image was acquired January 6, 2002, and is a color-coded display of a single thermal infrared band. The hottest areas are white, and colder areas are darker shades of red.

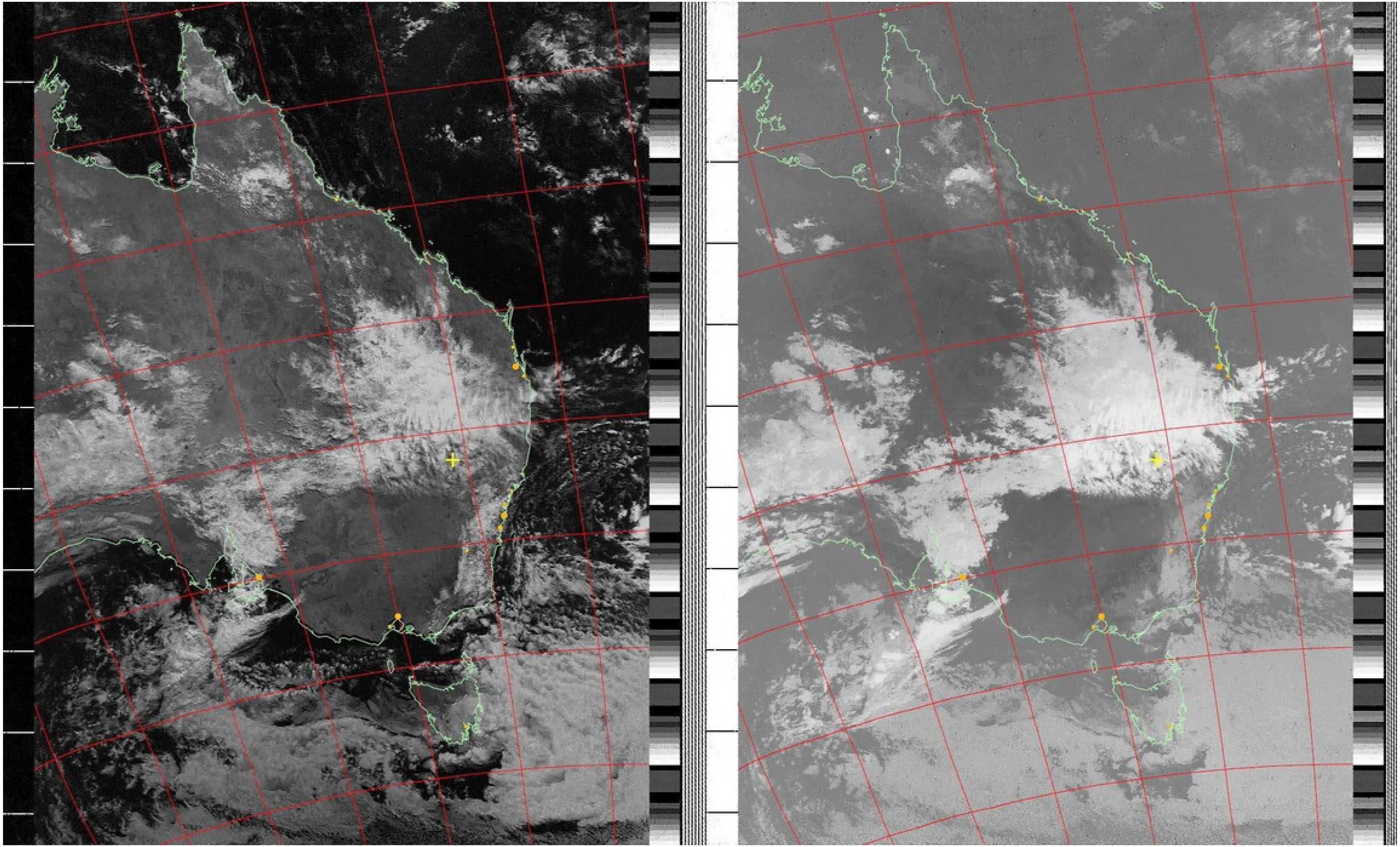

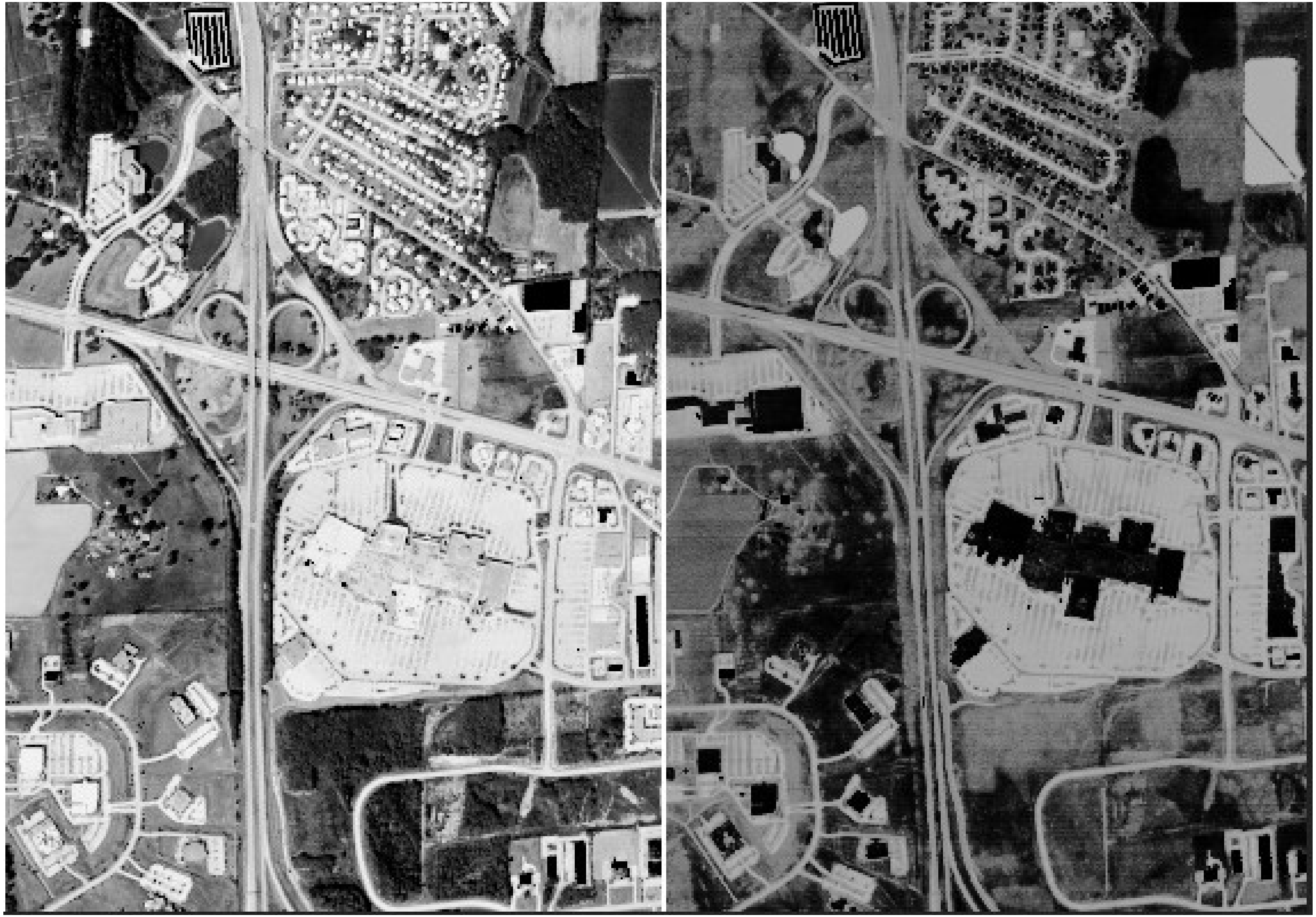

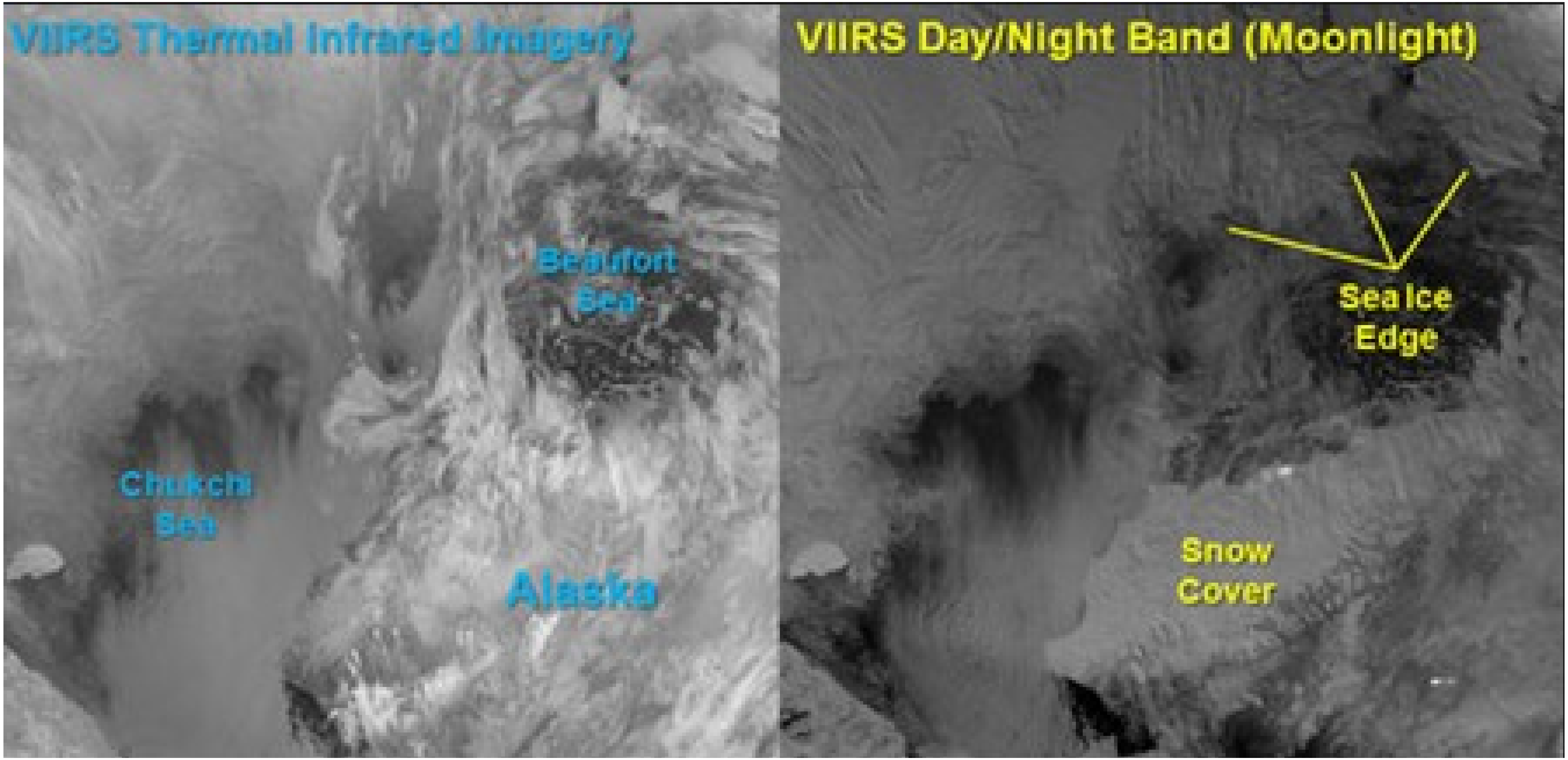
VIIRS Thermal Infrared Imagery
Beaufort Sea
Chukchi Sea
Alaska
VIIRS Day/Night Band (Moonlight)
Sea Ice Edge
Snow Cover

Day versus Night Image

Day

Night

Day image: Contrasts between heated buildings and streets and areas in shadow create a scene that resembles an aerial photo

Night image: Many streets are evident because, being asphalt paved, they absorp more heat and remain warmer through the night

Great Lakes -- Night

TM band 6 on Landsat

The land appears cool (darker tones) with little detail

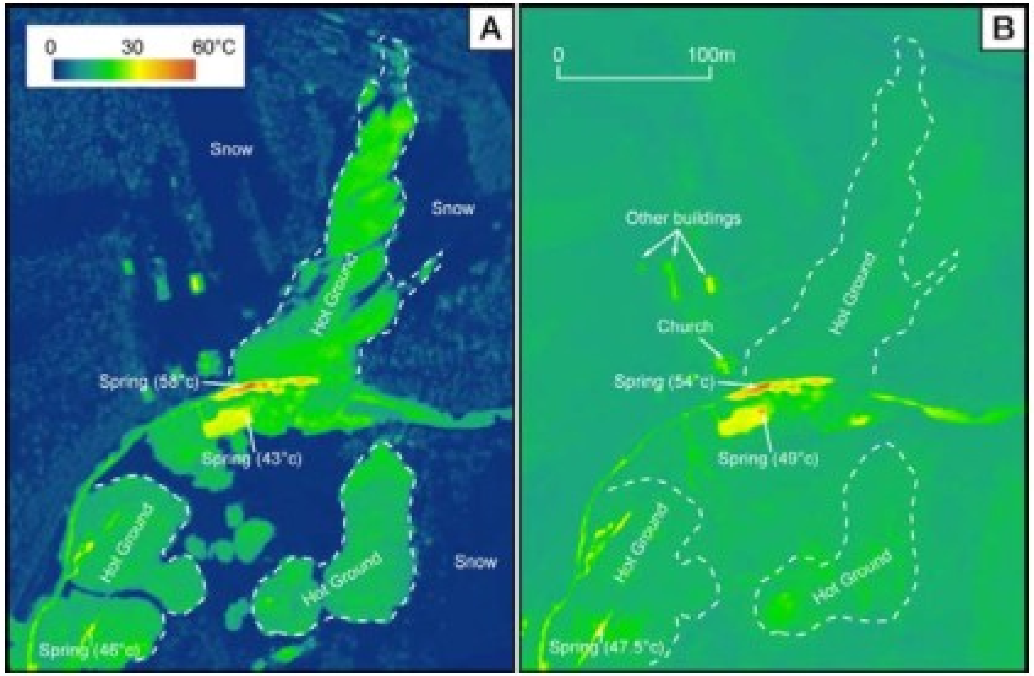

Figure 2 – Calibrated surface temperature data for part of Pilgrim Hot Springs acquired during winter 2011 (A) and fall 2010 (B) airborne surveys using a FLIR thermal camera. This data highlights the location of hot springs, hot pools and areas of heated ground as manifested in areas of anomalous snow melt in the winter 2011 data; from Haselwimmer et al., (2011).

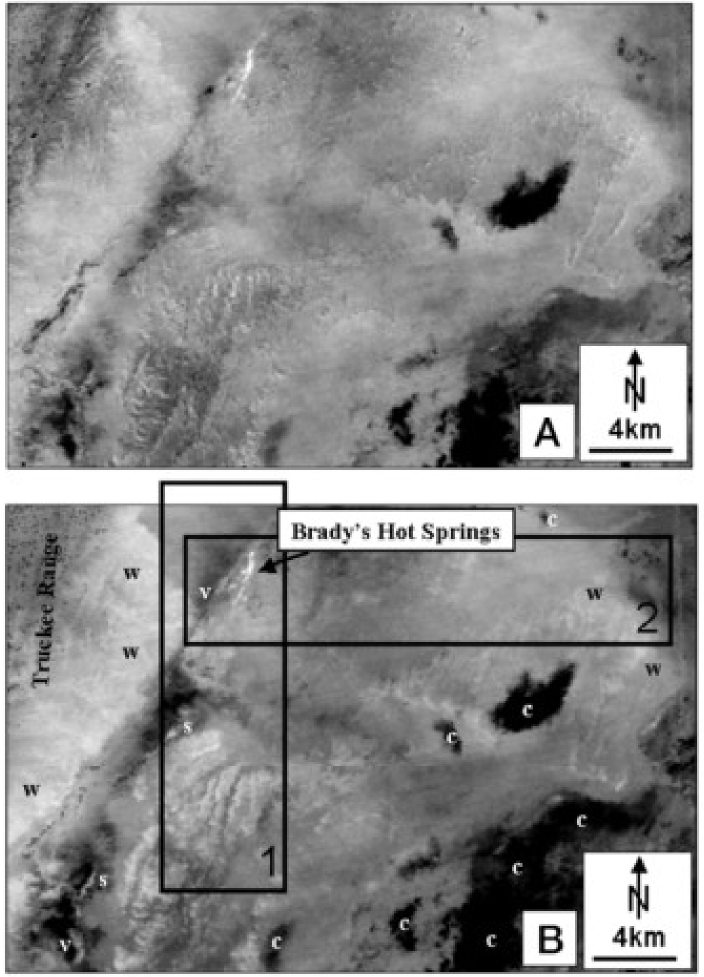

Figure 3 – ASTER day-night image for the Brady's Hot Springs area processed to minimize variations in temperature related to albedo, topographic slope/aspect, and thermal inertia (A) and unprocessed ASTER nighttime surface kinetic temperature (AST08) image (B). Around 34-53% of temperature variation in (B) has been removed in (A) as evidenced from the variances in temperature of the areas encompassed in boxes 1 and 2. This processing has resulted in the Fumaroles at Brady's Hot Springs being more readily discernible. Abbreviations: c = clouds, s = ground water springs, v = vegetation, W = 'warm' ground; adapted from Coolbaugh et al., (2007)

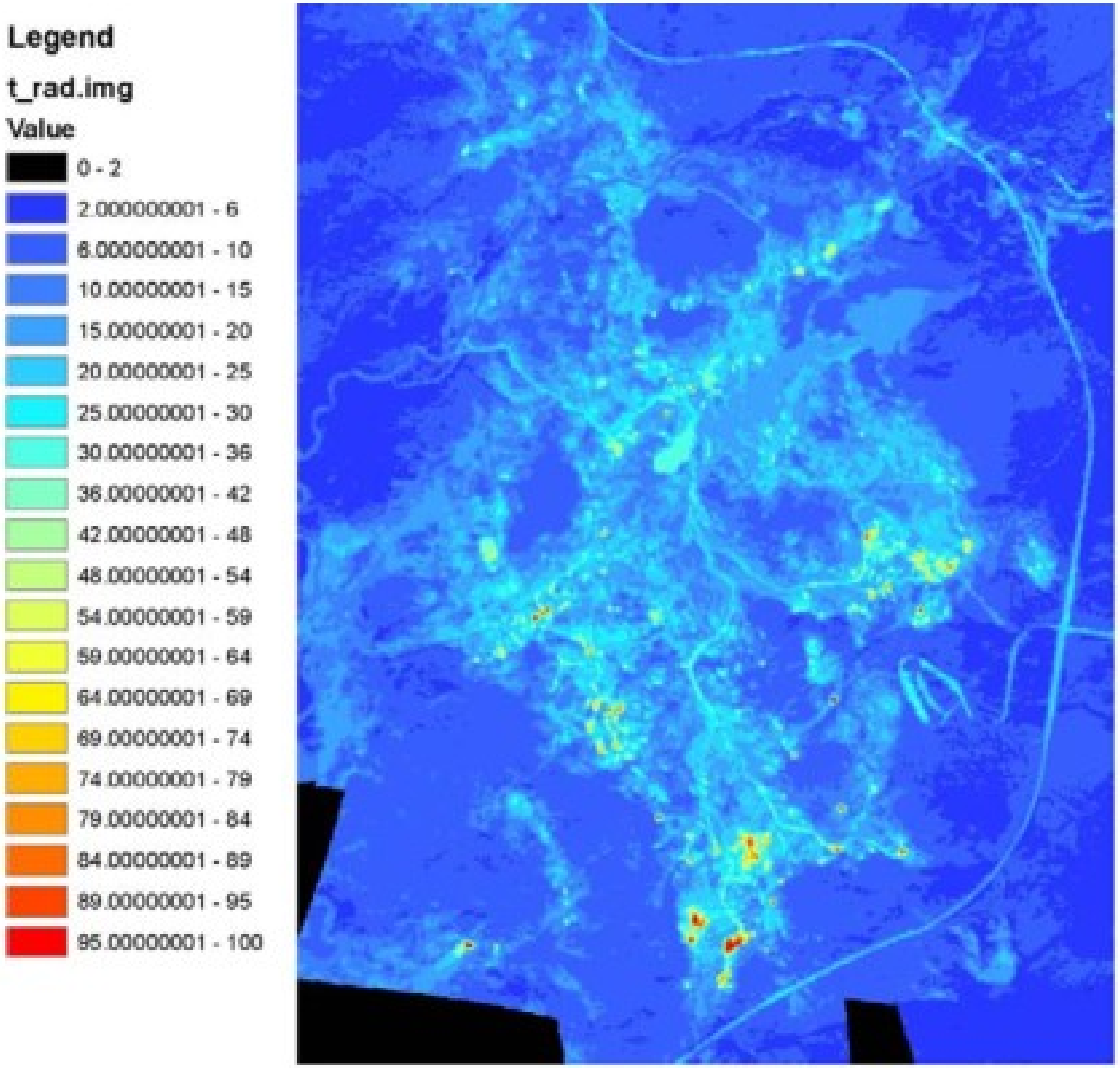

Figure 4 – Radiant temperature values (in degrees C) for Norris Geyser Basin acquired on October 06, 2005 between 1-3pm using ASD SpectraView system; from Seielstad and Queen (2009).

Thermal images will vary considerably in appearance depending on whether they are acquired during the warm part of the day or after a night of absence of the Sun and resultant cooling of the atmosphere as well as heat loss from the surface and shallow depths beneath.

This is evident in these two images of central Atlanta, GA. taken during the day (left, or top) and then just before dawn (right, or bottom). The thermal sensor was flown on an aircraft.

In the day thermal image, contrasts between heated buildings and streets and areas in shadow create a scene that resembles an aerial photo. But in the dawn image, differences in temperature have decreased sharply (no shadows), although a part of that image is brighter, representing a local "heat island" effect. Also, in the dawn image, many streets are evident because, being asphalt paved, they absorb more heat and remain warmer through the night.

Unlike remote sensing reflected light from surfaces in which only the topmost layers (a few molecular layers thick) are involved, thermal remote sensing includes energy variations extending to varying shallow depths below the ground surface. This takes time and is the normal consequence of heating during the day and cooling at night. The most critical consideration in analyzing and interpreting thermal data and imagery is that of knowing the physical and temporal conditions that heat the near surface layers. Over the seasons, minor shifts in the mean temperature in bedrock can occur to depths of 10 m (33 ft) or more. Solar radiation and heat transfer from the air significantly heat materials at and immediately below the surface during the day. Temperatures usually drop at night primarily by radiative cooling (maximum radiative cooling occurs under cloudless conditions), accompanied by some conduction and convection. During a single daily (diurnal) cycle, the near surface layers (commonly, unconsolidated soils) experience alternate heating and cooling to depths typically between 50 and 100 cm (20-40 in). The daily mean surface temperature is commonly near the mean air temperature. Observed temperature changes are induced mainly by changes during the diurnal heating cycle, but seasonal differences (averages and range) in temperature and local meteorological conditions also affect the cycle response from day to day.

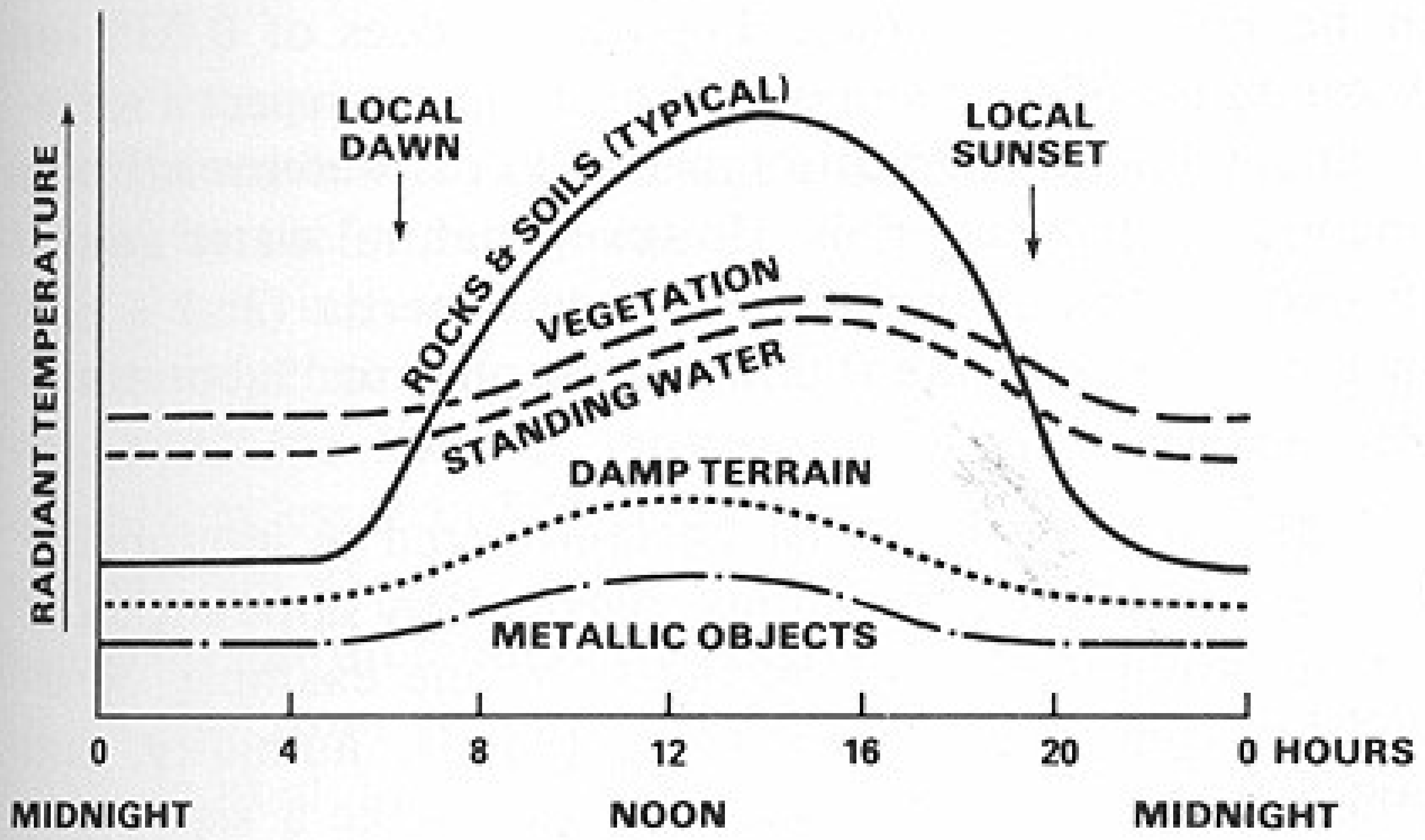
RADIANT TEMPERATURE
LOCAL DAWN
ROCKS & SOILS (TYPICAL)
LOCAL SUNSET
VEGETATION
STANDING WATER
DAMP TERRAIN
METALLIC OBJECTS
0
4
8
12
16
20
0 HOURS
MIDNIGHT
NOON
MIDNIGHT

DIURNAL CYCLE FOR REFLECTED SHORT-WAVELENGTH AND EMITTED LONG-WAVELENGTH ENERGY

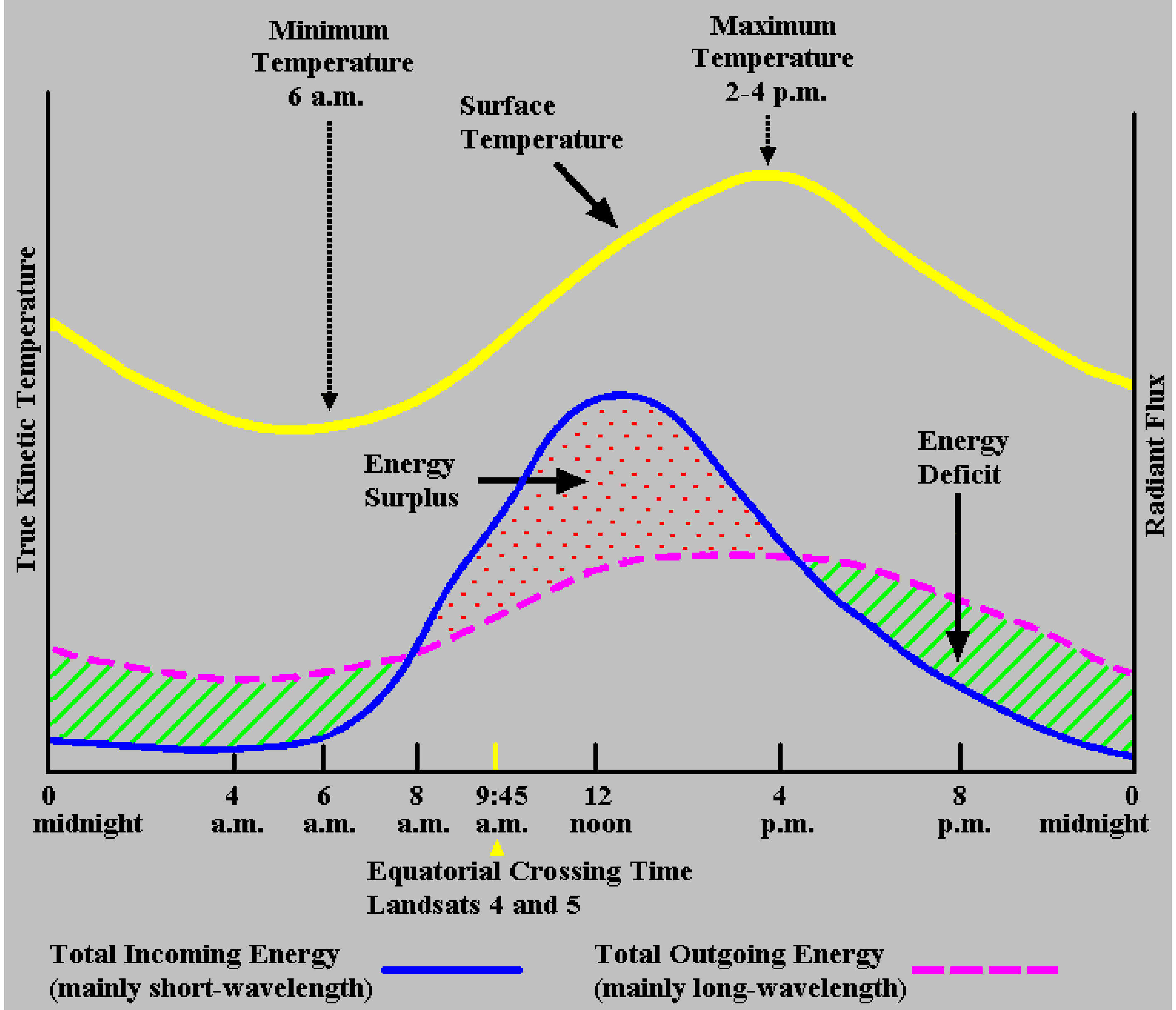

Source: Modified from Marsh and Dozier, 1981

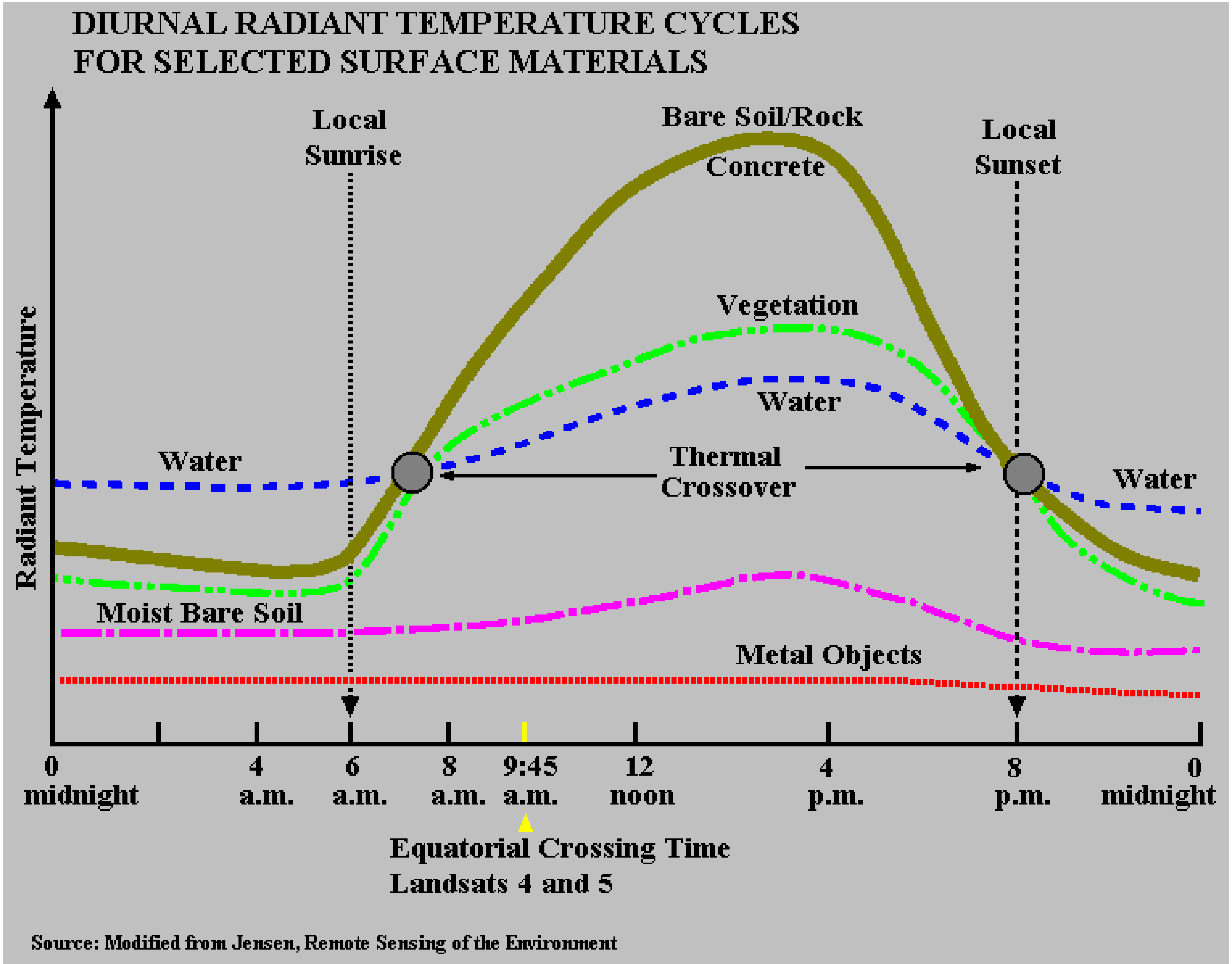
DIURNAL RADIANT TEMPERATURE CYCLES
FOR SELECTED SURFACE MATERIALS
Radiant Temperature
Local
Sunrise
Bare Soil/Rock
Concrete
Local
Sunset
Vegetation
Water
Water
Thermal
Crossover
Water
Moist Bare Soil
Metal Objects
0
midnight
4
a.m.
6
a.m.
8
a.m.
9:45
a.m.
12
noon
4
p.m.
8
p.m.
0
midnight
Equatorial Crossing Time
Landsats 4 and 5
Source: Modified from Jensen, Remote Sensing of the Environment

Timing of image acquisition

The urban heat island is considered to be a night-time phenomenon, since it is best developed a few hours after sunset when the rural surface cools rapidly and heat is extracted from the adjacent air. (Figure 1). The urban atmosphere on the other hand continues to be warmed by the man-made urban surfaces which have higher heat capacity and thermal inertia than rural surfaces. In high-rise areas, these radiatively active surfaces are extensive, and potential energy loss by outgoing long wave radiation is blocked by the urban canyon geometry, with low sky view factors.

- Thermography is a printing or imaging method.
- The term comes from the Greek words "therme," meaning heat and "graphos," meaning writing or drawing.
- The printing method, known as thermographic printing uses heat to create an image.
- The imaging method, known as thermographic imaging captures infrared energy emitted by the subject.

- Thermography is a technique for visualizing the temperature of surfaces by recording their emission of long-wavelength variation.
- This heat radiation is detected electronically and displayed with different colours representing different temperatures.
- Thermograms are used to check houses for heat loss, so their heat insulation can be improved.

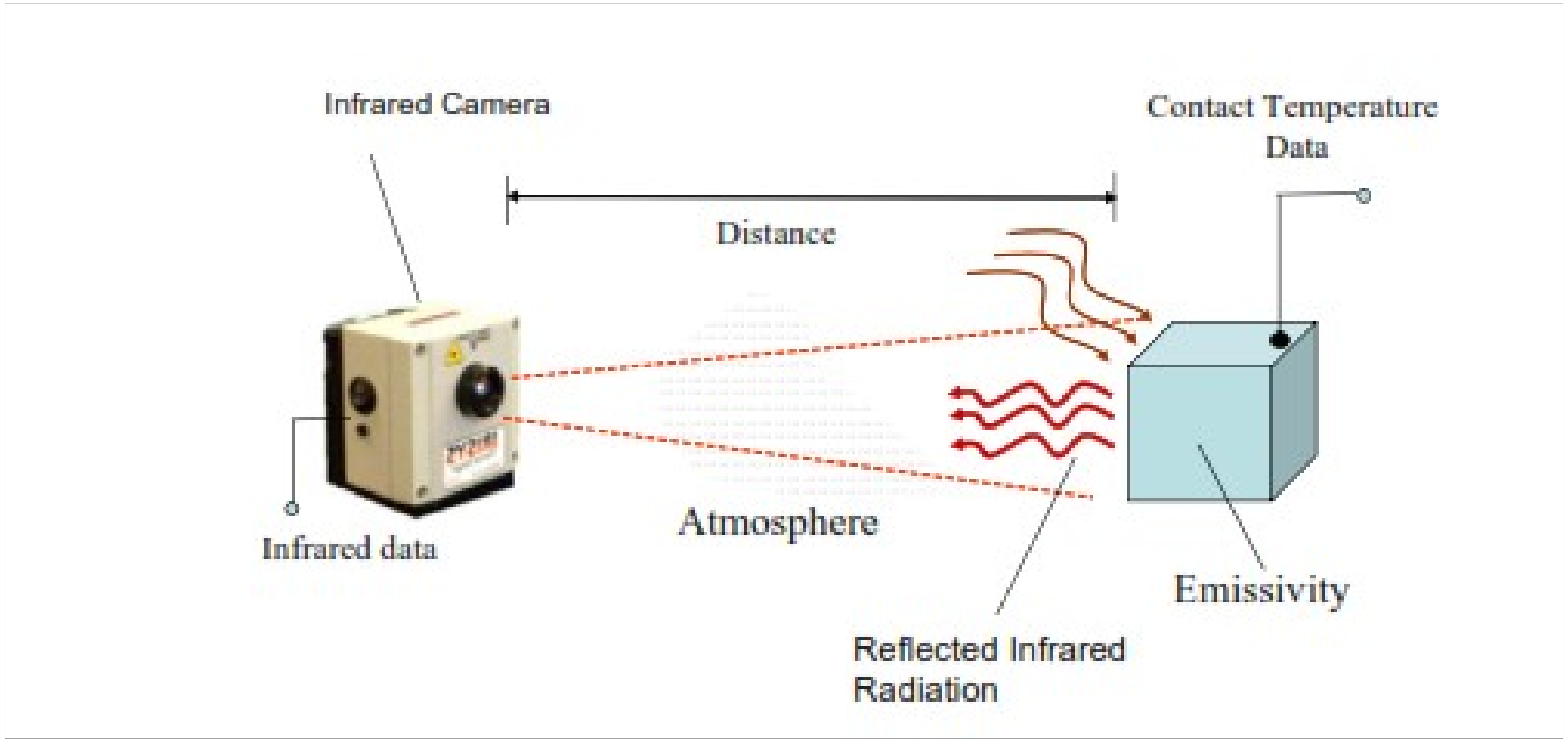
Infrared Camera
Contact Temperature Data
Distance
Atmosphere
Infrared data
Emissivity
Reflected Infrared Radiation

- Objects transfer heat by three means: conduction, convection and radiation.
- Conduction is the transfer of heat through solid objects.
- Convection is the transfer of heat through the movement of a fluid such as air and
- Radiation is the transfer of heat energy via electromagnetic radiation emitted by the object.

- The radiation emitted by the object includes the infrared radiation which can be detected by an infrared camera. Infrared radiation is emitted by every object above absolute zero.
- The amount of infrared emitted by the object is partly a function of the temperature of the object as described by Steffan-Boltzmann law. Infrared radiation is electromagnetic waves of a length between 0.7um and 1000 um.

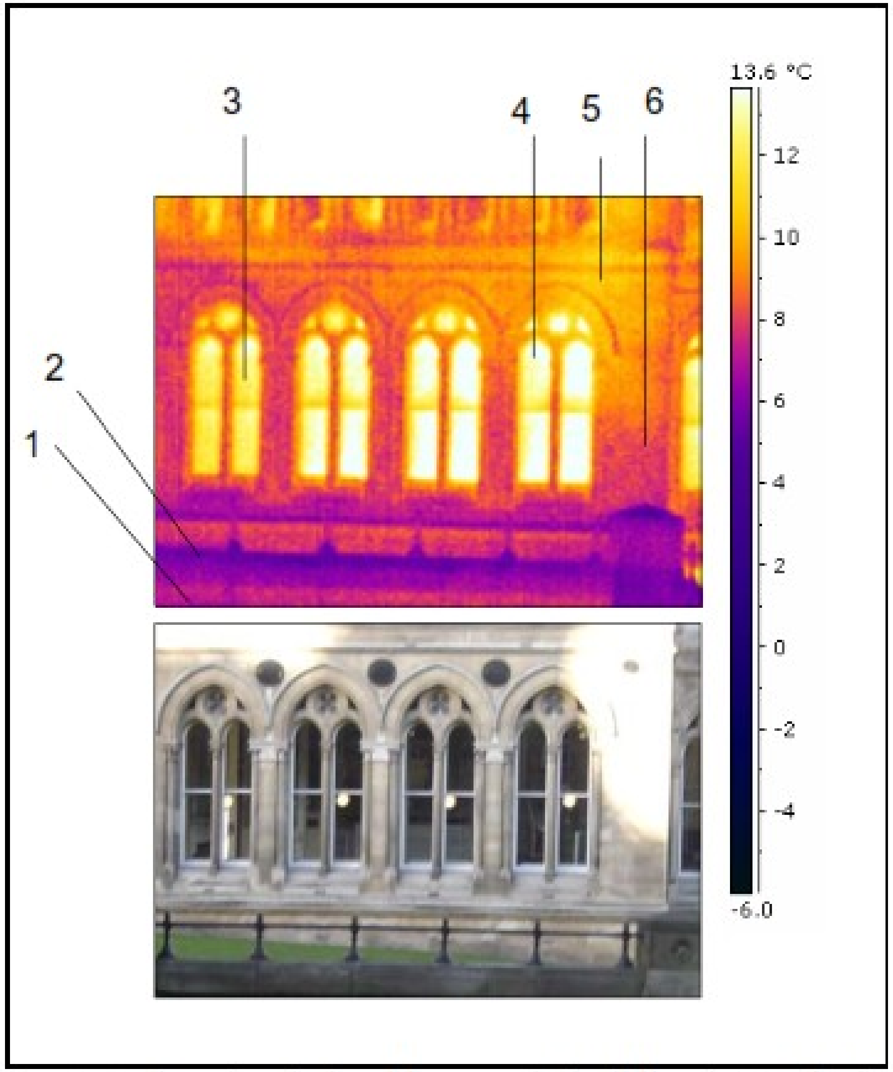
13.6 °C
3
4
5
6
2
1
12
10
8
6
4
2
0
-2
-4
-6.0

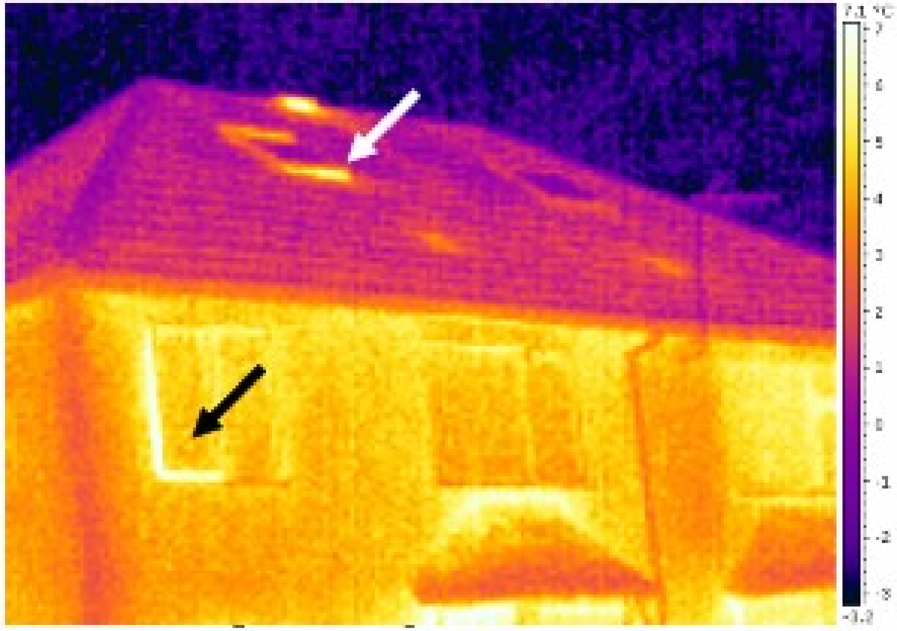

Real subsurface coal fire

Simulated surface coal fire

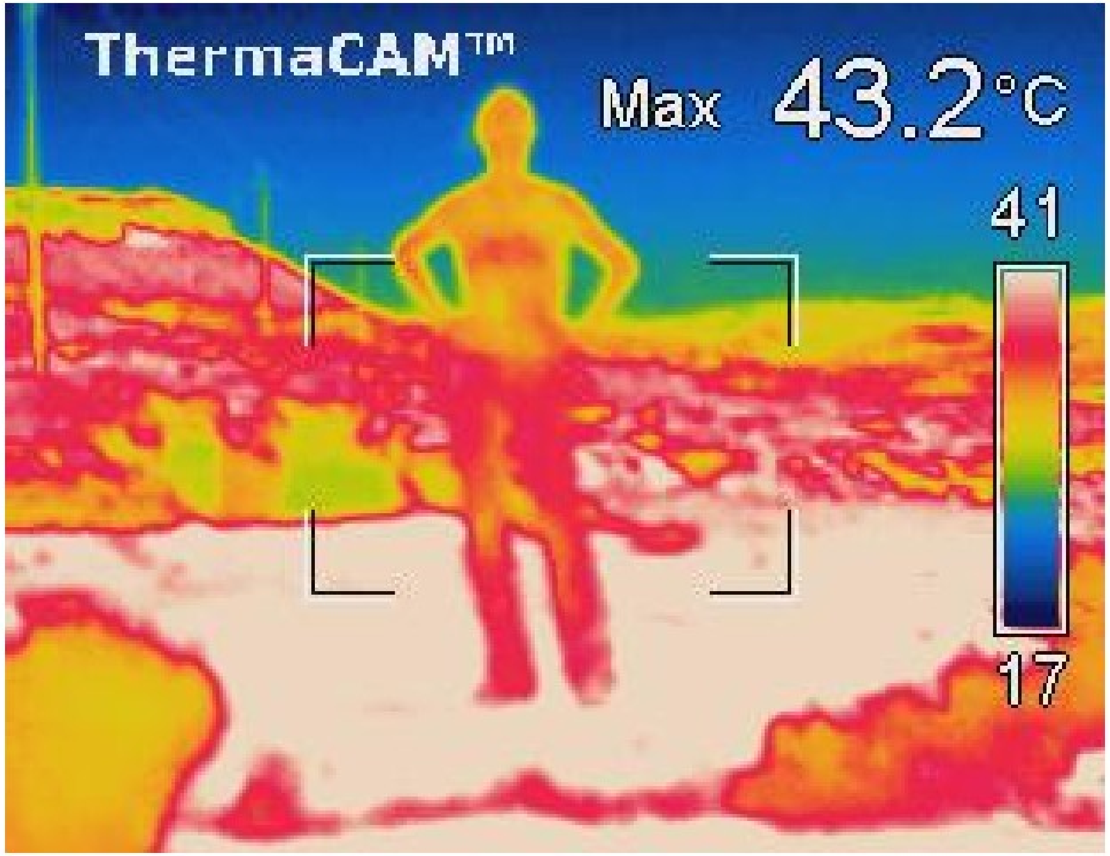

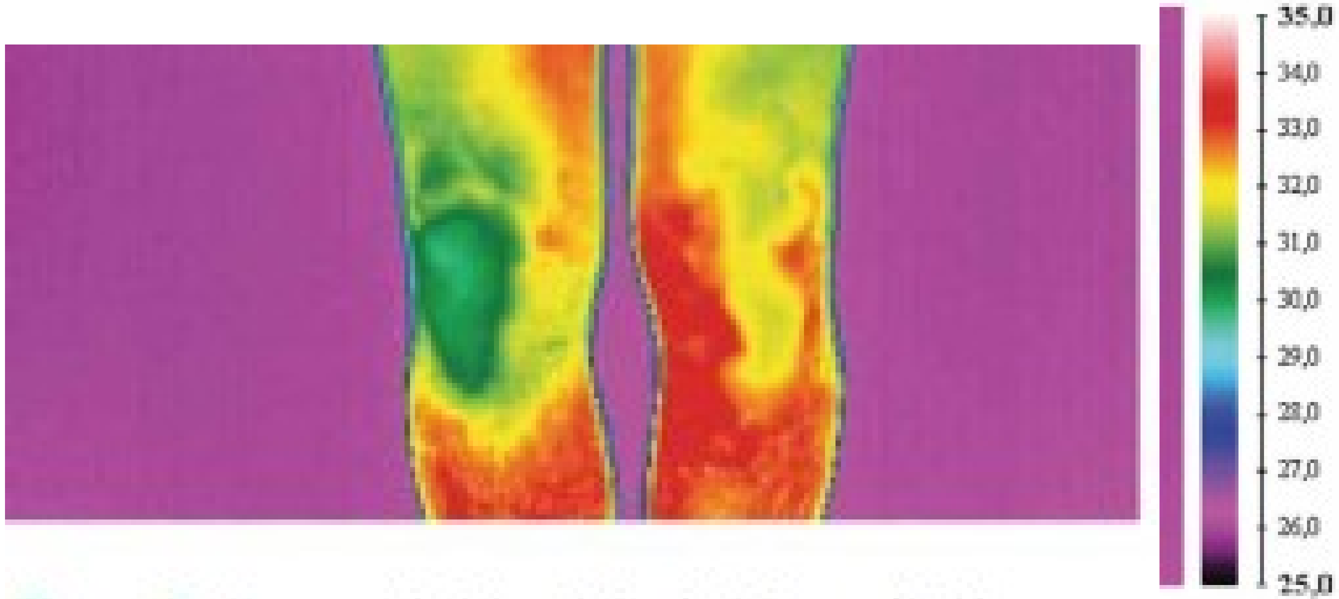

Figure 3. *Osteoarthritis of the left knee (left), tempe*

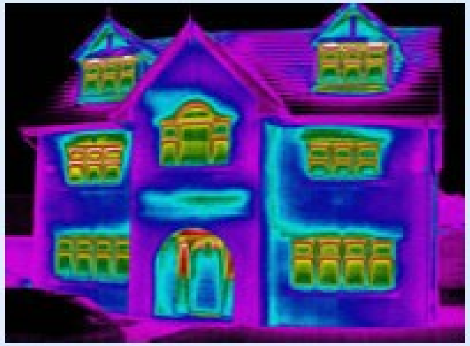

Thermal bridging, air leakage and air infiltration are all ways in which heat is lost or energy is wasted. We highlight these areas and give you recommendations on how to improve the thermal performance of your building.

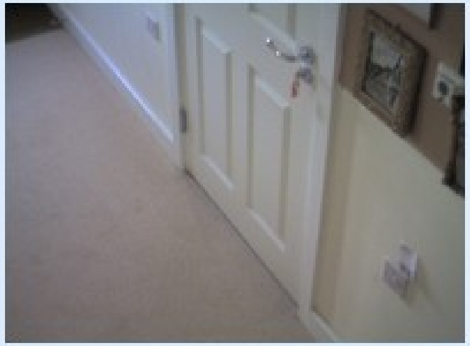

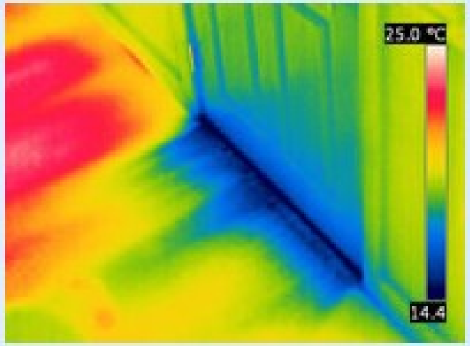

Air Infiltration or drafts can have a major impact on the heating within a property and can significantly increase heating bills. We are able to locate these areas and recommend actions to stop or restrict them.

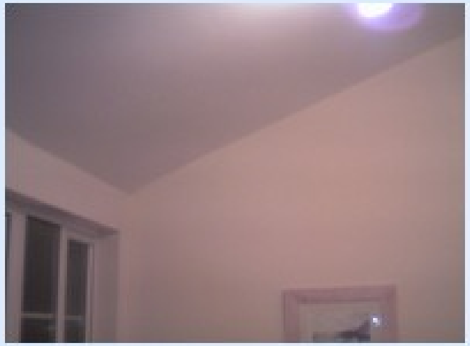

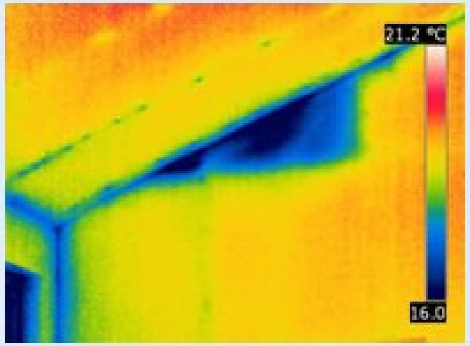

We are able to detect missing, sagged or wet areas of insulation within walls, structures and ceilings. These areas not only lose heat but can also allow condensation to form which can cause mould growth.

Thermal Expression of Coal Fires in EO Data

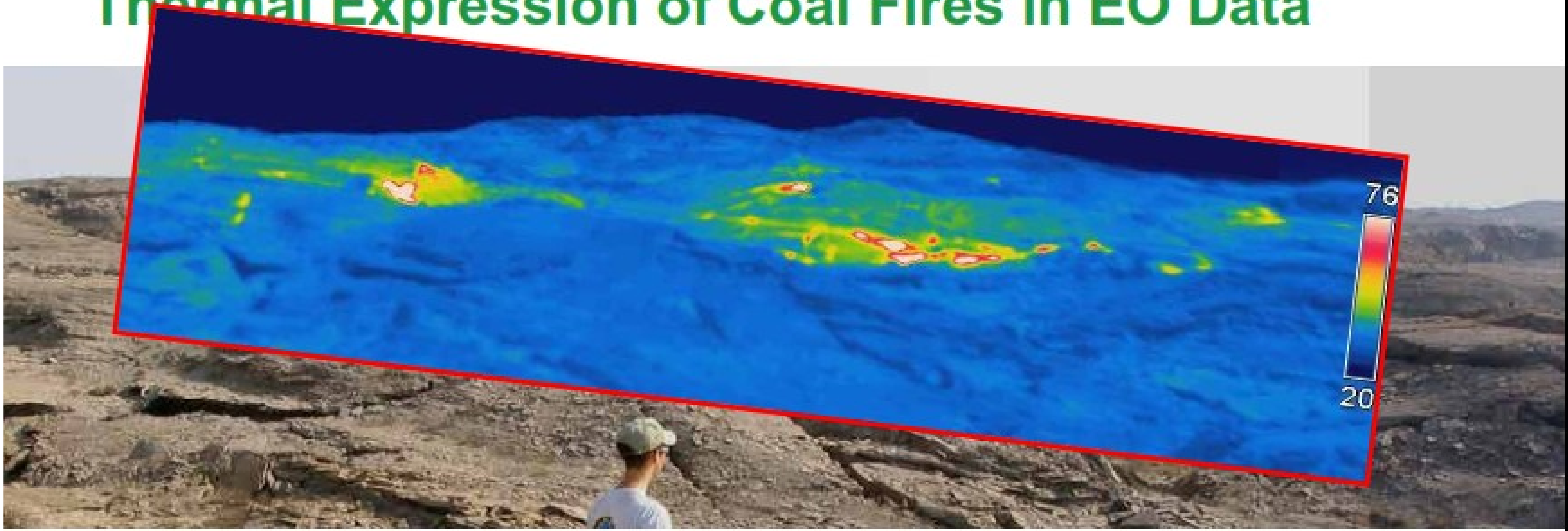

Radiation of real Materials

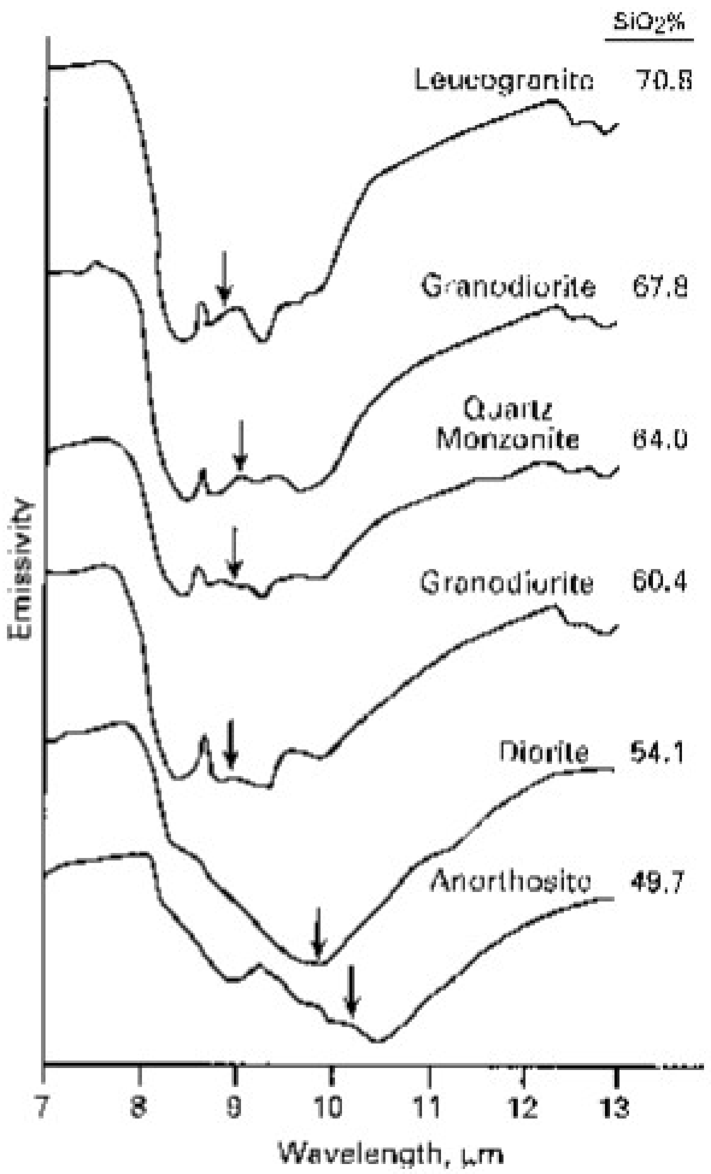

Emissivity spectra of different igneous rocks. Arrows show centers of adsorption bands. Spectra are offset vertically (Source: Sabins 1997).

DN to Radiance

1. **There are two formulas that can be used to convert DNs to radiance.**
2. **This method use depends on the scene calibration data available in the header file(s).**
3. **One method uses the Gain and Bias (or Offset) values from the header file.**
4. **The another method uses the LMin and LMax spectral radiance scaling factors.**

2.1.1. Gain and Bias Method

The formula to convert DN to radiance using gain and bias values is:

$$L_\lambda = gain * DN + bias$$

Where:

L_λ is the cell value as radiance

DN is the cell value digital number

gain is the gain value for a specific band

bias is the bias value for a specific band

The ENVI formula in Band Math will look like:

0.05518 * (B1) + 1.2378

using a scene specific gain value of 0.05518 and an offset value of 1.2378. In the Band Pairing dialog you should match B1 with the appropriate optical band.

2.1.2. Spectral Radiance Scaling Method

The formula used in this process is as follows:

$$L_\lambda = ((LMAX_\lambda - LMIN_\lambda)/(QCALMAX - QCALMIN)) * (QCAL - QCALMIN) + LMIN_\lambda$$

Where:

L_λ is the cell value as radiance
QCAL = digital number
$LMIN_\lambda$ = spectral radiance scales to QCALMIN
$LMAX_\lambda$ = spectral radiance scales to QCALMAX
QCALMIN = the minimum quantized calibrated pixel value (typically = 1)
QCALMAX = the maximum quantized calibrated pixel value (typically = 255)

$$L_{\lambda} = \frac{(R_{MAX} - R_{MIN})}{QCALMAX - QCALMIN} \times (DN - QCALMIN) + R_{MIN}$$

Where,

L_{λ}= Spectral Radiance at the sensor's aperture (w/m^{2*}sr*µm)

DN= Quantized calibrated pixel value (Q cal)

QCALMIN = Minimum quantized calibrated pixel value corresponding to LMINλ [DN] =1

QCALMAX= Maximum quantized calibrated pixel value corresponding to LMAXλ [DN] =255

However, QCALMAX for Landsat 8 is 65535

RMIN= Spectral at-sensor radiance that is scaled to Qcalmin (W/m2* sr * µm)

RMAX=Spectral at-sensor radiance that is scaled to Qcalmax (W/m2* sr * µm)

Conversion of Spatial Radiance into Temperature Kelvin: Step 2

ETM+ thermal band data converted to spatial radiance, which is a more physically useful variable. Assuming surface emissivity =1 (USGS, 2001), the following equation is used to convert radiance to temperature Kelvin:

$$T = \frac{k_2}{In[(k_1 \div L_\lambda) + 1]}$$

Where, T= Temperature in Kelvin, L_λ= Spectral Radiance

Conversion of Temperature Kelvin to Degree Celsius: Step 3

The temperature in Celsius was calculated using the equation

T (°C) =T-273.13

Where, T (°C) = Temperature in Celsius, T= Temperature in Kelvin, 273.13= Zero Temperature Kelvin

CONSTANTS (UNITS)	K1 (W/m2* sr * µm)	K2 (Kelvin)
L7 ETM+	666.09	1282.71
L8 TIRS	774.89	1321.08

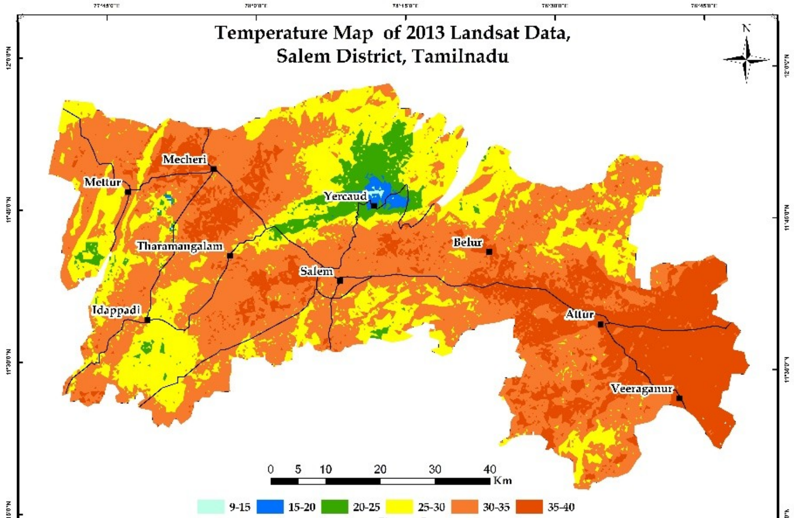

Figure: 5

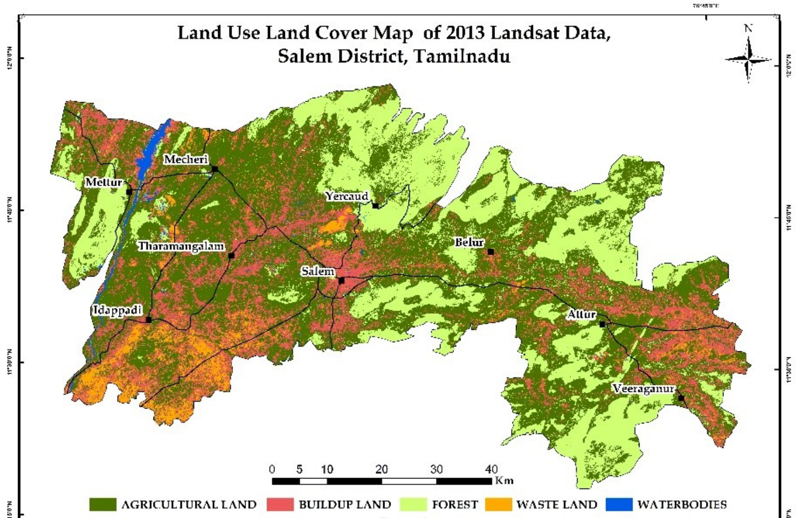

Figure: 3

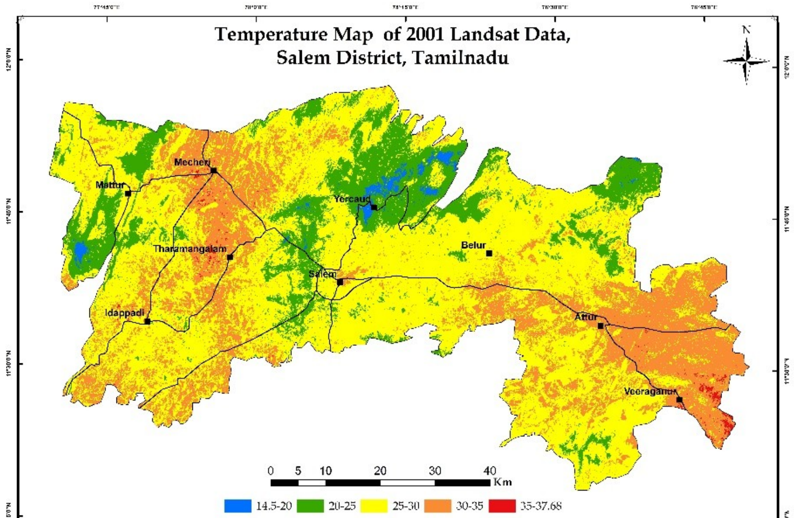

Figure: 4

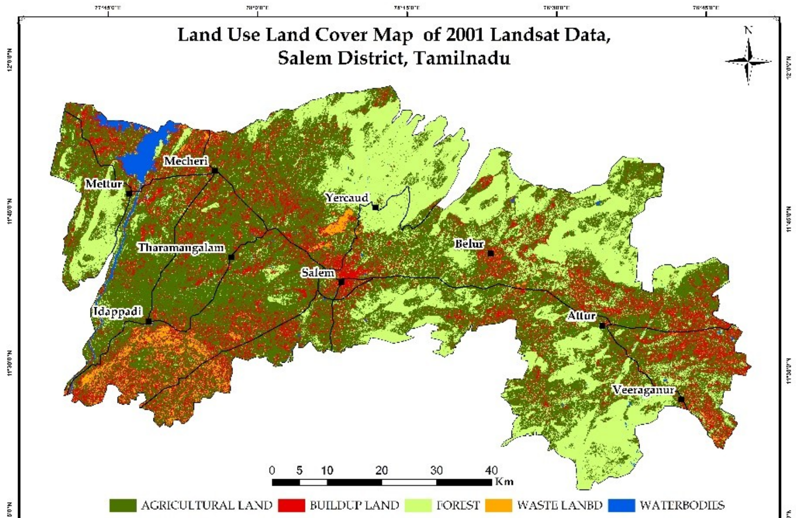

Figure: 2